INTERNATIONAL JOURNAL OF
COASTAL, OFFSHORE & ENVIRONMENTAL ENGINEERING IJCOE Vol.9/No. 4/Autumn 2024 (30- 41)

Available online at: www. Ijcoe.org

Investigating spectral and experimental methods in predicting wind waves in the southern regions of Iran (case study: Asalouye port)

Homayoon Ahmadvand[1*], Ali Sheykh bahai[2], Amer Kaabi[3], Dariush Abolfathi

*1- *PhD in Marine Physics, Khorramshahr University of Marine Sciences and Technology, Iran*
2- Responsible director of the International Quarterly Journal of Coastal and Offshore Engineering
3- Petroleum University of Technology, Department of Basic Sciences and Language (Abadan)
4- Assistant Professor, Payam Noor University, Department of Natural Geography

ARTICLE INFO

Article History:
Received: 15 Jun 2024
Accepted: 15 Oct 2024

Keywords:
wind waves
duration
significant wave height
wave spectrum

ABSTRACT

sea level rise due to wind are one of the most important phenomena in marine environments that are effective in the coastal and offshore processes. This paper discusses methods to evaluate the accuracy of experimental and spectral methods in predicting wind waves in Asaluyeh port. Empirical methods including SMB, SPM, CEM and Jonswap and Spectral methods include Bretschneider, Mitsuyasu, Pierson-Moskowitz, Jonswap, ISSC spectrum were considered to evaluted the mentioned waves. The results show that Jonswap method among experimental methods in duration of 6 hours is the most appropriate method to determine the wave profile in Asaloyeh port. Furthermore by comparing spectral methods it was found the Bretschneider, Mitsuyasu and Pierson-Moskowitz spectrum show lowest error in the calculation of H_{m0} nd f_p. To better match the measured spectra, their coefficients were corrected and after height value was calculated using each spectrum. Then, using corrected and uncorrected spectra, directional spectra of the region were plotted.

1. Introduction

The presence of waves caused by wind and sea level rise near the coastal strip can be effective in increasing the energy of coastal waves. Especially in areas where root and tidal waves are also present in these areas [1]. Recently, various methods have been used to obtain the values of the significant wave height and the wave period as characteristics of the wave energy base on real data observation [2]. Raj N and et al, predicted significant wave height for sustainable wave energy [3]. Hashemi and shahidi Extracted of the significant wave height from synthetic HF radar data acquired on a floating platform [4]. Ardhuin and Carlo retracking of altimeter waveforms yields fluctuations in wave height and sea level. The result shows that Retracking of altimeter waveforms yields fluctuations in wave height and sea level, correlated at the scale of the effective footprint[5]. Accurate modelling of multimodal sea states is of primary importance for most of offshore and coastal activities, such as wave energy device optimization, maritime design practice and for safety at sea. Sartini and Antonini have researched spectral wave climate and wave systems analysis of the French Atlantic Ocean. Furthermore swell system and local topography are evaluated quantitatively on the whole area The results of this research have shown that the two-faceted shape of this region and the interruption of the seas in this region cause the change of the entire wave directional spectrum[6]. In the last 5 years, the experimental study of wave height , crest and the trough distribution of the directional irregular waves that are produced on a sloping surface have been studied [7]. In the ports of Iran, especially the southern ports of Iran, research has been done on waves and renewable energy, one of the sources of which is wind [8]. Goharnejad et all evaluated the energy of waves in the Persian Gulf under the influence of the region's climate [9]. Furthermore Vafaeipour Sorkhabi et al investigated the behavior of quay walls under random waves through experimental methods. The study used walls with vertical geometrical form, which were exposed to sea random waves under the JONSWAP spectrum. A neural network model was developed using the feedforward method with the backpropagation algorithm to analyze the time series of water surface level and strain[10].

Waves caused by the wind in the coastal strip can affect the fish and aquatic environment[11,12].

Considering that fish and marine animals are caught on the shores of Asalouye port, and also the relationship between weather conditions and the height of strong sea waves [13], therefore, in this research, it is supposed to predict local and online wind waves in this area using experimental models and Suggested spectrum.

In addition, according to the breakwaters built in Asalouye port and the necessary measures to repair or maintain them, it is necessary to access the statistics of the waves recorded in that area, so in terms of the engineering principles of marine structures, it is necessary to investigate and analyze the spectrum of these types of waves[14]. Lee et al studied joint Probability Distribution of Significant Wave Height and Peak Wave Period Using Gaussian Copula Method [15]. Therefore, the study of the index wave period is still one of the important topics in marine science and engineering studies.

Considering the numerous offshore and onshore constructions, drillings and oil and gas platforms in the region, the demand for a reliable metocean forecast system has highly increased in recent years. For methods of forecasting SMB, SPM, CEM and Jonswap methods can be noted. In each of these methods by comparing of tmin with wind duration, continuous time limit or fetch limited condition was determined, then the values Hm0 and TP were obtained. In particular, Jonswap, Pierson-Moskowitz, Mitsuyasu and Bretschneider and ISSC spectral methods can be cited which using the calculated spectral parameters m0, m2 and m4 of every one of them, Hm0, H1/10 , Tz and Tc and Tp parameters are calculated [16,17].

Mohammad Pakhirehzan, et al, The numerical study of winter shamal wind forcing on the surface currents and the wave field in Bushehr Offshore using MIKE21 model [18]. The significant wave height and wave propagation speed for the period of Winter Shamal Wind in comparison with the days prior to the wind show significant changes.

The latest research from the study of the wave that has been published on the topic of the wave goes back to the article of Wang et all. In this study, the Assimilating wave spectrum and wave height Assimilation based on from satellite observations have been investigated and compared. When comparing with the buoy measurements, spectrum assimilation demonstrated superior effectiveness in improving mean wave period (MWP) compared to SWH assimilation [19]. Ahmadvand et al used empirical and spectral methods in predicting wind wave characteristics in Amir Abad port [20]. Stanislav Kotaška studied the spectral analysis and empirical formulaof wind wave parameters of Haline water resources under limited wavelength conditions [21]. This means, the proposed methods in this research, which include experimental and spectral methods, are not obsolete yet. Therefore, in this research according to the climate changes of a region, this issue has been re-examined.

In the following, the coefficients of the spectral models were corrected and the directional spectrum of this port was calculated and drawn using the effective spectrum in this area. In no other research, the directional spectrum of wind waves in Asalouye port has not been investigated.

2.Material and methods

2.1. Empirical methods of wave prediction

A simple method to predict the parameters waves are using by empirical relationships. These methods which are provided based on dimensional analysis, generally, calculate the significant wave height and peak periods based on input parameters such as wind speed, wind direction, duration. In Table 1 some of theses methods mentioned. In the following we will refer to these relations (It is mentioned in the appendix)

- In all methods if the actual time is greater than tmin, Wave growth, is limited by the fetch and based on relations at the last column of the table, wave height and period (Ts and Hs) values can be calculated. In SMB method when the real duration is smaller than the tmin, limited duration condition dominates and equation (1) used to determine the effective fetch [22].

$$X = \frac{U^2}{g} exp\left(\frac{1.76A - 0.369 - \sqrt{0.084A^2 - 1.3A + 6.776}}{1.51} \right)$$

$$A = \ln t - \ln\left(6.59 \frac{U}{g} \right)$$

(1,2)

- In the SPM method, wind stress1 is related directly to the wave growth. To determine the vertical profile of wind stress and hence wind speed, differences in air-water temperature, sea surface roughness and friction velocity should be considered. All of these factors with wind stress UA are taken into account by SPM and its value is calculated according to the following equation [16].

$$U_A = 0.71 U_{10}^{1.23}$$

(3)

- In the CEM method, wind shear speed u* is in meters per second and is calculated from following equation [17].

$$u_* = U_{10} \{ 0.001 (1.1 + 0.035 U_{10}) \}^{0.5}$$

(4)

In the CEM method if the duration limited condition dominates, for the computation of the equivalent fetch, equation (4) is used.

$$\frac{gX}{u_*^2} = 5.23 \times 10^{-3} \left(\frac{gt}{u_*} \right)^{\frac{3}{2}}$$

(5)

[1] - U_A

In SMB and Jonswap methods for calculation of the effective fetch, a limited region within ± 45 on each side of main wind direction should be considered that consist of 15 radials from the wave station at intervals of 6 degrees, and extending until they first intersect the shoreline. The component of length radial in a direction parallel to the wind direction is measured. The effective fetch is calculated from weighted average of length of radials using following equation [22]:

$$X = \frac{\sum X_i \cos\theta_i}{\sum \cos\theta_i}$$

(6)

While X_i is the length of each radial and θ_i is the angle of each of each radial. In SPM and CEM methods for calculation of the effective fetch, a limited region within ±15° relative to the main wind direction is considered.

2.2. Wave spectrum

The power spectral density represents the effect of frequency on the signal's power [23]. The spectrum of a signal can be viewed as a function that tells us what portion of the power is carried by what frequency components – it is a function of the spectral power density. In general, for a frequency spectrum equation (9) is presented. A and B are regulator of the shape and spectrum scale parameters respectively and can be defined as a producer function of wave, wave height and wave period.

$$E = \frac{A}{f^5} exp\left(-\frac{B}{f^4}\right)$$

(7)

In the past decade based on data collected and analysis conducted, spectrum for several different conditions are presented. In Table 2 refers to a number of them [24, 25] (table is in Appendix). One of the important methods for determining the profile of the wave spectrum is the use of spectral moment. The spectral parameters H_{m0} and T_p can be (8) to (9) achieved.

$$H_{mo} = 4\sqrt{m_o}$$

(8)

$$T_p = f_p^{-1}$$

(9)

In the above relationships H_{m0} and T_p are wave height and peak period.

2.3. Directional spectrum

the directional wave spectrum applied for separating wind sea and swell from directional wave spectra in finite-depth waters [26]. So use of directional wave spectrum in the advanced models is essential. Wave models are often one-dimensional directional models modified by a function of frequency and the wave direction.

$$E(f,\theta) = E(f)G(f,\theta)$$

(10)

E(f,θ) is directional spectrum, E(f) is frequency spectrum and G(f,θ) is non-dimensional spreading function. Since the modified frequency spectrum to the directional spectrum does not change the total energy density, the following relationship is established:

$$\int_{-\pi}^{\pi} G(f,\theta)d\theta = 1$$

(11)

$$m_o = \int_0^{\infty}\int_{-\pi}^{\pi} E(f,\theta)d\theta\, df$$

(12)

θ usually is clockwise its origin considered to be zero in direction of dominant wind and its practical range is from $-\pi/2$ to $\pi/2$. Based on wave data analysis and theoretical analysis, several publications related to the directional spreading function $G(f,\theta)$ provided. One of the relationships is PNJ and the formula is as follows [27]:

$$G(f,\theta) = G(\theta) = \begin{cases} \frac{\pi}{2}\cos^2\theta & |\theta| \le \frac{\pi}{2} \\ 0 & |\theta| > \frac{\pi}{2} \end{cases}$$

(13)

3. Study area

The study area is located in Asaloye region at the southern coast of Iran in the Persian Gulf (Fig. 1). Asaloyeh is an important economical region in the Persian Gulf because it is close to the Pars gas field and marine transportation activities. Wind and wave data were gathered by Iranian National Center for Oceanography (INCO), respectively. The recorded wave data was collected at $27^o49'94''$ and $52^o59'0''E$ and water depth at the wave station was about 25 m. The period of data collection was from 2002 to 2003. Statistics of wave and wind characteristics are indicated in Table 3. Table 3 shows that the average wind and wave directions are from the southeast and south directions, respectively.

Another important subject is the possible existence of swells. Since the Persian Gulf is a semi-enclosed sea, swells cannot easily propagate into it from the Indian Ocean due to the existence of Strait of Hormuz.

4- Result and discussion

4.1. predicting H_{m0} by experimental formula

In order to use the wave prediction equations, status of deep or shallow water has been verified. Therefore, using the ratio d/L= 8.41, were found that deep water conditions are prevailing. Also, using the relations listed in Table 1, and by assuming t= 6, 9 and 12 hours, results of calculations are shown in figures 2 to 5.

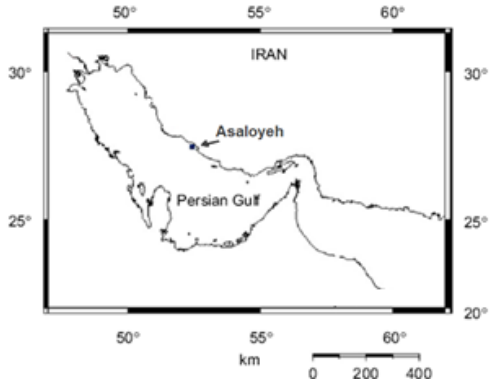

Fig. 1. Map of Persian Gulf at Asalouye port.

Table 3: Maximum, minimum and average values of the used data.

Parameters	Min	Average	Max
Significant wave height (m)	0.011	0.582	3.24
Wave direction (deg.)	37.91	258.3	349.2
Wave peak period (s)	1.845	4.32	7.37
Wind speed (m/s)	0.124	5.12	16.9
Wind direction (deg.)	0.255	228.9	359.9

Predicted values in each of the above methods, compare to the measured values are with error. Thus for compare and evaluate each of them, mean square root values are calculated in Table 4. Comparison between the calculated values of using Jonswap method for wind with of 6 hours duration showed maximum accuracy in estimation of wave height and period. The results showed that SMB and SPM method with duration of 12 hours calculate more

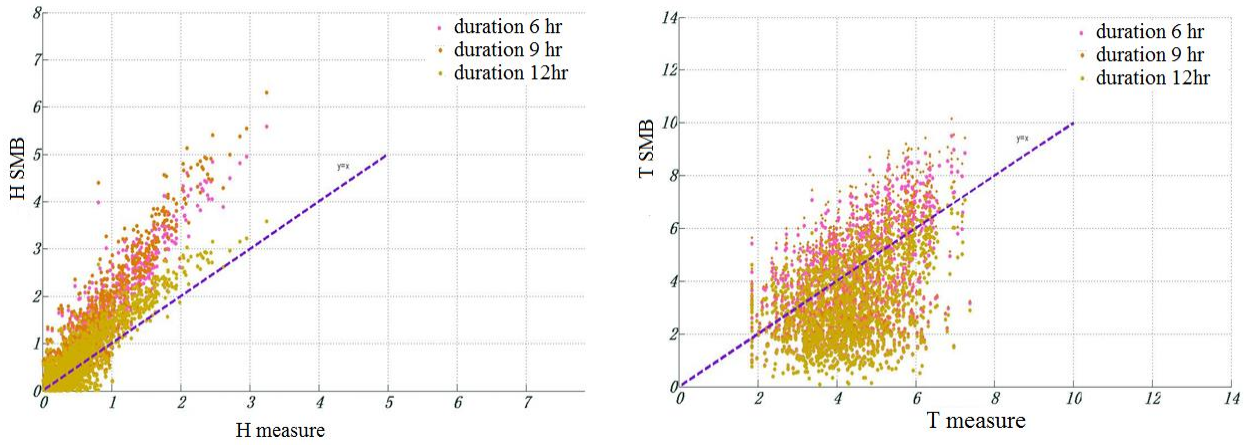

Figure 2: Comparison of measured and predicted values of wave height and period by using SMB formula

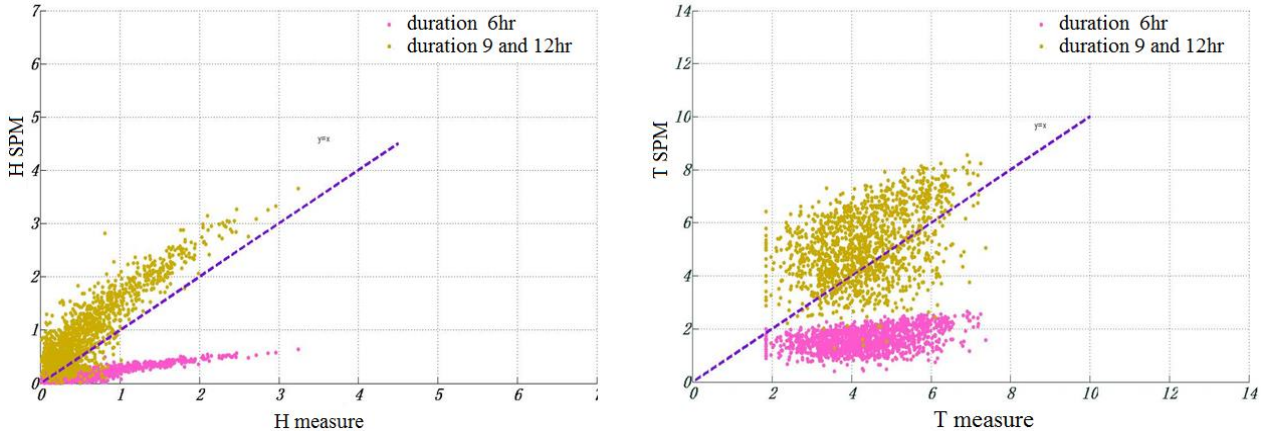

Figure 3: Comparison of measured and predicted values of wave height and period by using SPM formula

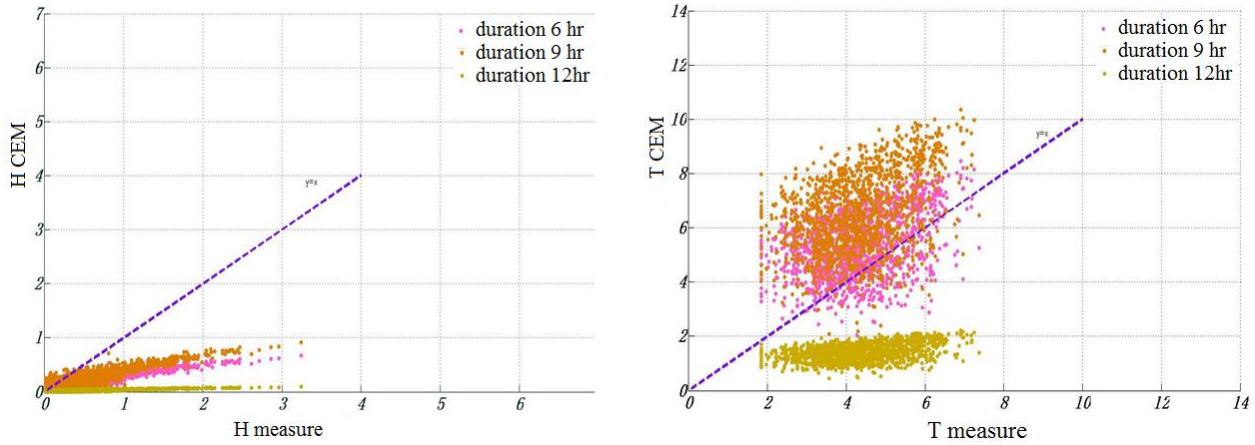

Figure 4: Comparison of measured and predicted values of wave height and period by using CEM formula

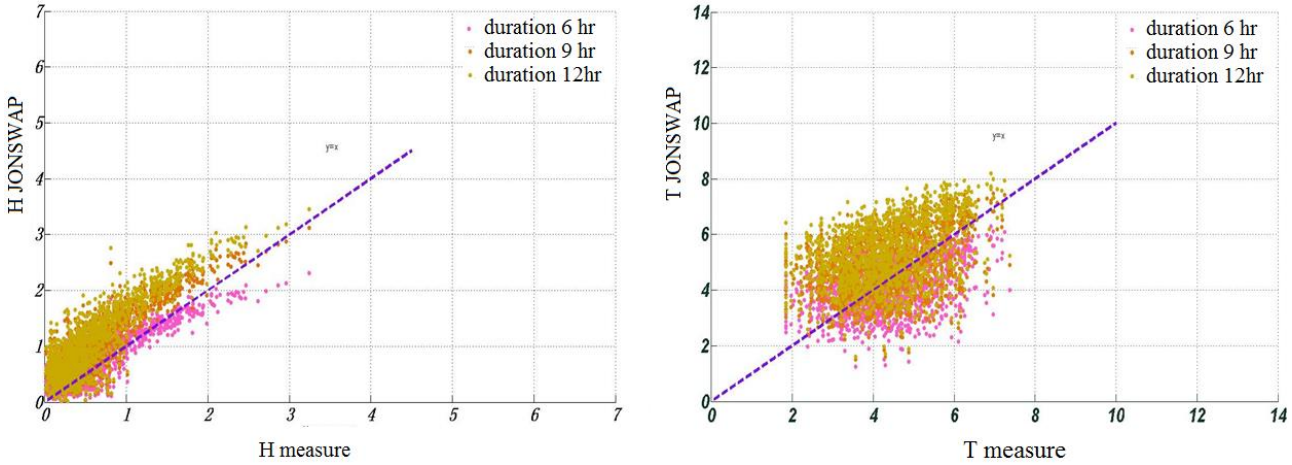

Figure 5: Comparison of measured and predicted values of wave height and period by using Jonswap formula

Table 4: Comparison of the mean square root values of Hs and Ts in experimental methods of wave prediction

		duration		
	parameter	***6hours***	***9hours***	***12hours***
SMB	H_s	87.77	100.16	45.53
	T_s	42.92	43.98	42.38
SPM	H_s	75.40	63.79	63.79
	T_s	65.08	34.30	43.30
Jons wap	H_s	44.99	68.39	73.89
	T_s	29.89	29.66	34.66
CEM	H_s	72.06	62.62	96.16
	T_s	35.59	57.80	69.21

accurate values of the wave height and period. While the Jonswap for 6 hours duration, predicts the wave height and period with the lowest error. In the CEM method for duration of 9 hours and 6 hours respectively, minimum error in the calculation of wave height and period will result. So with an overall view of the table we can say, Jonswap method with duration of 6 hours, show the least amount of error in calculating the wave height and period.

4.2. Spectral analysis of data

To plot the selected spectrum, first the Δf value calculated based on the frequency difference between maximum and minimum divided by number of data, And then adding Δf each time to minimum frequency, the frequency values and frequency spectral density values are calculated. Also for plotting the measured spectrum using the relationship S = a^2 / 2, S values for each data which expressed with specifications ai and fi can be plotted. In Figure (6) the spectra are plotted without fitting. As can be seen many fluctuations in the energy spectrum, but the location and maximum size has been determined to be appropriate. To reduce its volatility, the chart in the MATLAB software using the first order Gaussian fitted which which results is shown in the figure (7).

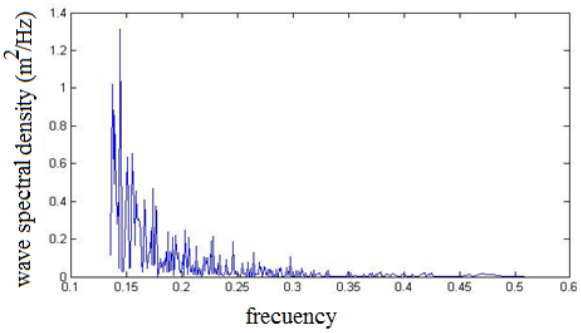

Figure 6: Spectrum of the measured data

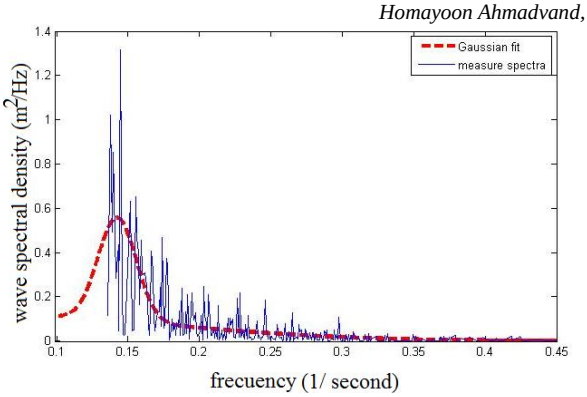

Figure 7: The fitted spectral density data

In order to compare each spectrum with the plotted spectra, Using Table 2, in the figure (8) spectrum are plotted and compared with the measured spectrum. It can be concluded that the spectra of the Pierson-Moskowitz and Bretschneider Mitsuyasu spectrum are closely fitted.

4.3. Comparison of the measured spectrum with selected spectra

For analyze and evaluate each of the spectra, we compared the calculated values of H_s with calculated value from measured spectrum. So that based on $H_{mo} = 4\sqrt{m_0}$ equation and assumption that in deep water $H_{mo} = H_s$ significant wave height of each of the Pierson-Moskowitz, Mitsuyasu and Bretschneider has been calculated. Also for calculation the H_s time series based on zero up-crossing spectrum is plotted. The values of the each frequency interval of measured spectrum in equation (20) have been replaced. The values of phase function chosen uniformly of a random number in the range of 0 to 2π (Figure 9).

$$\eta = \sum_{n=1}^{\infty} a_n \cos(w_n t + \varphi_n) \quad (13)$$

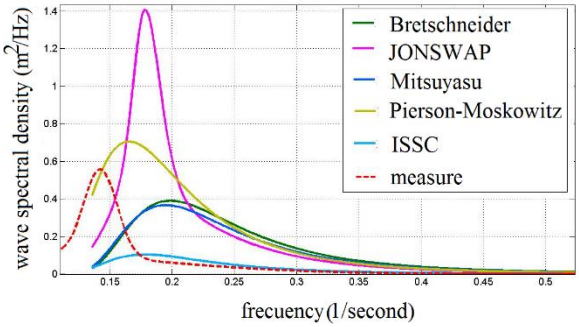

Figure 8: Comparison of spectral energy density of measured data with theoretical spectrum

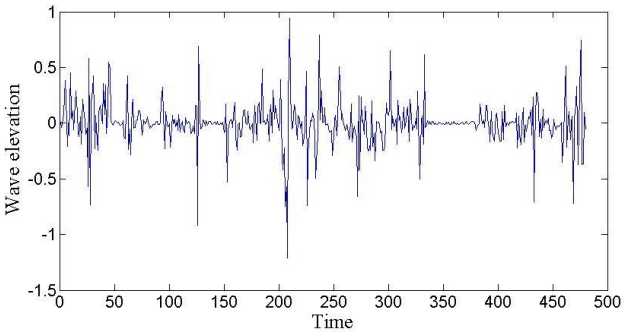

Figure 9: profile of the sea level using the values of wave height and frequency selected from measured spectra

Results using the mentioned methods listed in Table 5. The results show that Mitsuyasu and Pierson-Moskowitz spectrum predict the wave height with minimum and maximum error respectively,

Table 5: Comparison of calculated and measured Hs in Mitsuyasu - and Pierson Moskowitz and Bretschneider spectrum

Spectrum	Pierson-Moskowitz	Bretschneider	Mitsuyasu
Hs (m)	1.015	0.849	0.815
Error of measurement H_S (%)	35.57	13.39	8.5

4.4. Correction of spectral relations of Mitsuyasu, Pierson-Moskowitz and Bretschneider

Mazaheri et al have also shown that the wave coefficients can be modified and the use of modified wave coefficients can be used to express the wave behavior in the northern waters of the Persian Gulf with higher accuracy [28].

Pierson-Moskowitz, Bretschneider and Mitsuyasu spectra with little difference have the good agreement with measured spectra. In order to match and more consistentency of Pierson-Moskowitz, Mitsuyasu and Bretschneider spectrum by the measured spectrum, their relationship as shown in Table 6 was calibrated to improved the results. In Figure 10 and Table 7 the results of these corrections is shown.

Table 6: corrected spectral relations of Mitsuyasu, Pierson-Moskowitz and Bretschneider

spectrum	Spectrum relation	description

Pierson-Moskowitz	$S(f)=\frac{3.362}{16}H_s^2\, f_p\, f^{-5}\, exp\left(-\frac{5}{4}\left(\frac{f_p}{f}\right)^4\right)$	$T_p=1.65\overline{T}$
Mitsuyasu	$S(f)=\frac{4298\times10^{-8}}{K^{0.3}}\frac{g^2}{f^5}exp\left[-0.99.6K^{-1.23}\left(\frac{f_u}{g}\right)^{-4}\right]$	$K=\frac{g\,F}{u^{1.37}}$
Bretshneider	$S(f)=0.116\left(\frac{\overline{H}}{gT^2}\right)^2\frac{g^2}{f^5}exp\left[-0.178\left(\frac{1}{\overline{T}\,f}\right)^4\right]$	---------

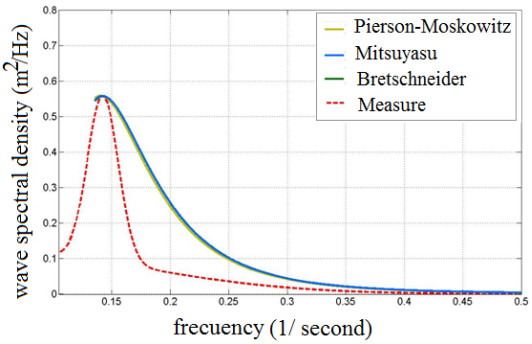

Figure 10: plotted Spectra Pierson-Moskowitz, Bretschneider and Mitsuyasu and after correction of relations

Lowest frequency that each of these spectra plotted are near the peak of the wave. For the spectrum at frequencies lower than the peak frequency, each of modified spectra, according to the figure 11, has fitted with Gaussian functions. In this figure minimum frequency is shown in shape of a point. Comparing the calculated errors values, wave height spectrum is calculated by the modified Pierson-Moskowitz More accurate than the other two spectra. Therefore the spectral parameters of the region using the mentioned spectra calculated H_{m0}=0.81 m and f_p= 0.14 (1/s).

Table 7: Comparison of significant wave height measurement error in each of the modified spectrum

spectrum	Pierson-Moskowitz	Mitsuyasu	Bretschnieder
Calculated H_S	0.81	0.8252	0.8265
Error of calculation (%)	8.56	10.21	10.39

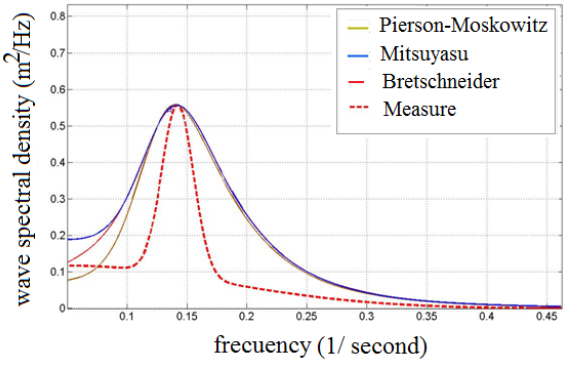

Figure 11: Gaussian fitted corrected spectra Pierson-Moskowitz ,Mitsuyasu and Bretschneider.

4.5. Directional spectrum of the wave

To plot directional spectrum using the relationship $E(f,\theta)=E(f)G(f,\theta)$ the function of the frequency $E(f)$ based on the frequency spectrum Pierson-Moskowitz, Mitsuyasu and Bretschneider and the angular part $G(f,\theta)$ based on the theory of PNJ is considered. Directional spectra of the region using modified and unmodified Pierson-Moskowitz, Bretschneider and Mitsuyasu Spectra have been plotted in Figures 12 to 15. Figure 12 shows the directional spectrum of the Pierson-Moskowitz spectrum similar to its frequency spectrum; less of the minimum frequency is not defined.

4.6. Comparison with previous research

Shamshirband et al, has predicted the height of the index wave in Asalouye region. In this research, soft models have been compared. The results demonstrate that all the models generally provide sound predictions. Due to the high level of variability in the bathymetry of the study area, implementation of the nested grid with different Whitecapping coefficient is a suitable approach to improve the efficiency of the numerical models.

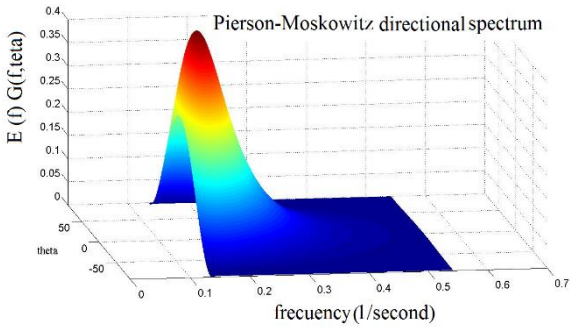

Figure 12: Pierson-Moskowitz directional spectrum, before the correction.

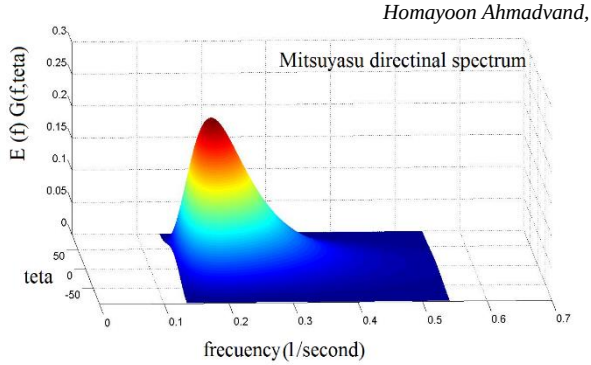

Figure 13: Mitsuyasu directional spectrum before the correction

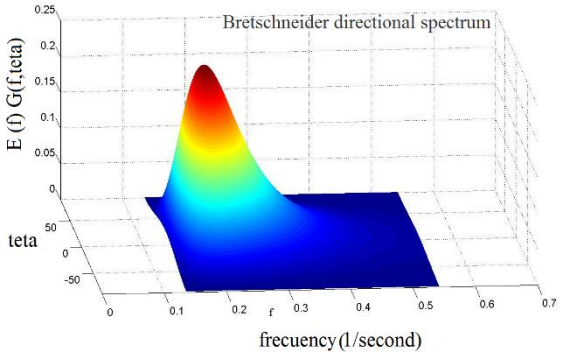

Figure 14: Bretschneider directional spectrum before the correction

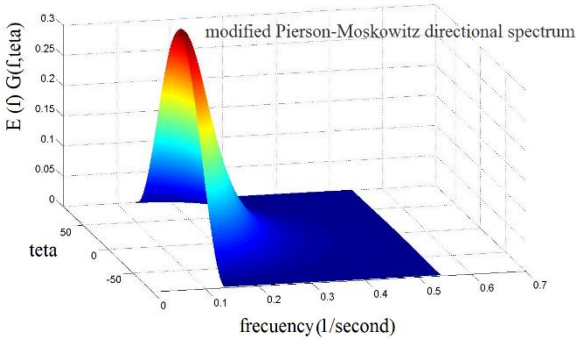

Figure 15: modified Pierson-Moskowitz directional spectrum

Performance on the ML models do not differ remarkably even though the ELM model slightly outperforms the other models. Figures (16) show the results of each of these models [29].

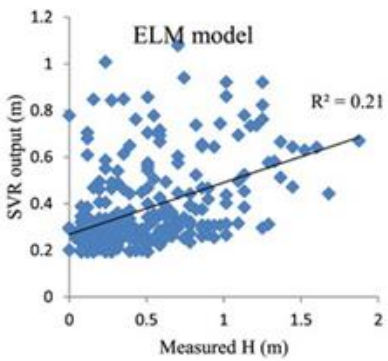

Figure 16 : The modeling results of Shamshirband et al. (2019) in predicting the height of waves in Asalouye region by soft computing

By comparing the results of Shamshirband research with the present research, it can be concluded that the best experimental model, which is the Jonswap model of this research, in predicting the wave height, is actually stormy and strong winds with higher accuracy than any of the soft models proposed in the shamshirband research.. This is despite the fact that in the researsh Shamshirband et al forecast is related to the online prediction and it is expected to have a lower accuracy.

Boyd and weaver was created parametric solver which incorporates four different wave height formulations (SMB, SPM, TMA, CEM) and can be used to create an ensemble average of parametric results. With validation from an ADCP deployed in the domain, the parametric models produced an average accuracy within 6% for wave height. This model also accurately simulates tropical storm wind events including variability in wind speed and direction with an average global accuracy of within 12.9% compared to SWAN [30]. Kotaška et al, concluded that the SMB model is the most accurate among the experimental models with an RMSE of 0.02 in online prediction in the deep water region [21]. So It is possible to predict with Jonswap's formula with an accuracy of 0.44 in Asalouye port, the data were collected in areas that were in deep water conditions. This difference in accuracy can be applied to the results of forecasts calculated in the lead time hours.

In the research of Najarpour et al., using adcp data, have shown the dominant spectrum of this region is in good agreement with the Janswap wave spectrum. In this research, it has been shown that with higher accuracy, the dominant spectrum of this region is closer to the Pierson-Moskowitz wave spectrum after the parameterization of the wave spectrum coefficients [31].

4.7. Conclusion

Assimilating observation data in to wave models can significantly improve the numerical simulation accuracy of ocean waves. This research focuses on the use of experimental and spectral methods in predicting wind waves in Asalouye port. The most important results of this research can be listed as follows:

- According to the past results in wave forecasting, it can be mentioned that experimental models have still maintained their validity in predicting wave height and in some cases where there is no access to marine measuring devices, these valid methods can be used with high predictive accuracy. It was used to evaluate the height and period of wind-induced waves in the region asalouye.
- In general, comparing performed show that Jonswap method for duration of 6 hours more accurately estimates the wave height and wave period. For durations of 6 and 9 hours the Jonswap empirical formula provided the most accurate estimation of

wave height (Hm0) with an average of RMSE = 0.44 m. Furthemore SPM and SMB methods for 12 hours duration, are considered most useful.

--The results show that the spectral proposed method has a high accuracy for identifying wave parameters shuch as wave period and significant wave height which is a re-emphasis on past results. in addition the spectral analysis of data showed that Pierson-Moskowitz, Mitsuyasu and Bretshneider spectrum with slight differences are close to the spectrum measured. So in the end it became clear that with the correction of their relationship Hs in the lowest range of errors is calculated by Bretshneider.

-It is noteworthy that the spectrums that are discussed in this study, all are suitable for deep water condition. With waves of deep water to the area with an average depth or less, time changes in the form of spectrum will take place. In this case use of TMA spectrum recommended that is modified Jonswap spectrum and by the depth and frequency-dependent coefficient of φ (f,h) is amended. This spectrum serves as a basis for simulating oscillatory waves and their impact on shore protection structure design.

- In the past research, it has been shown that in the northern sea areas of Iran (Caspian sea), the spectrum of wind waves has a double peak. This issue has been studied due to the return of waves from the coastal strip as well as the swell waves formed in the coastal zone. This is despite the fact that in the areas of the southern coasts of Iran, the spectrum of computational waves does not show such a thing and wave period sea had had lower 10 s. However, sometimes strong winds have been present in this area and the spectrum shown does not indicate the presence of swell waves, and all the waves recorded by marine devices are all the presence of local wind and local waves of the region.

Acknowledgement

The authors are thankful to the Ports & Maritime Organization, Iran for data used in this study.

References

[1] Barnes AT, Becker JM, Tagarino KA, O'Reilly WC, Siegelman M, Thompson PR, Merrifield MA. Rising sea levels and the increase of shoreline wave energy at American Samoa. Scientific Reports. 2024 Mar 2;14(1):5163.

[2] Verdejo H, Awerkin A, Kliemann W, Becker C, Chávez H, Barbosa KA, Delpiano J. A Dynamic Stochastic Hybrid Model to Represent Significant Wave Height and Wave Period for Marine Energy Representation. Energies. 2019 Mar 7;12(5):887.

[3] Raj N, Prakash R. Assessment and prediction of significant wave height using hybrid CNN-BiLSTM deep learning model for sustainable wave energy in Australia. Sustainable Horizons. 2024 Sep 1;11:100098.

[4] Hashemi S, Shahidi R, Gill EW. Extraction of the significant wave height from synthetic HF radar data acquired on a floating platform. IET Radar, Sonar & Navigation. 2023 Nov;17(11):1639-45.

[5] Ardhuin F, De Carlo M. Along-track resolution and uncertainty of altimeter-derived wave height and sea level: re-defining the significant wave height in extreme storms. Authorea Preprints. 2024 Apr 19.

[6] Sartini L, Antonini A. On the spectral wave climate of the French Atlantic Ocean. Ocean Engineering. 2024 Jul 15;304:117900.

[7] Xu J, Liu S, Li J, Jia W. Experimental study of wave height, crest, and trough distributions of directional irregular waves on a slope. Ocean Engineerigdng. 2021 Dec 15;242:110136.

[8] Rashidi Ebrahim Hesari A, Andi S, Farjami H. Study of internal waves in the Persian Gulf using field data and satellite images. International Journal Of Coastal, Offshore And Environmental Engineering (ijcoe). 2019 Nov 1;4(4):9-16.

[9] Goharnejad H, Nikaein E, Perrie W. Assessment of wave energy in the Persian Gulf: An evaluation of the impacts of climate change. Oceanologia. 2021 Jan 1;63(1):27-39.

[10] Vafaei Poursorkhabi R, Ejlali RG, Naseri A, Hosseinchi Gharehaghaji A. Experimental Study on Assessing Interaction of Quay Walls and Random Waves Using Artificial Neural Network. International Journal Of Coastal, Offshore And Environmental Engineering (ijcoe). 2023 Nov 1;8(4):1-8.

[11] Roulston MS, Ellepola J, von Hardenberg J, Smith LA. Forecasting wave height probabilities with numerical weather prediction models. Ocean Engineering. 2005 Oct 1;32(14-15):1841-63.

[12] Szewczyk TM, Morro B, Díaz-Gil C, Gillibrand PA, Hardwick JP, Davidson K, Aleynik D, Planellas SR. Interactive effects of multiple stressors with significant wave height exposure on farmed Atlantic salmon (Salmo salar) welfare along an inshore-offshore gradient. Aquaculture. 2024 Jan 30;579:740184.

[13] Kumar P, Yadav A, Sardana D, Prasad R. Extreme wave height response to climate modes and its association with tropical cyclones over the

Indo-Pacific Ocean. Ocean Engineering. 2024 Mar 15;296:116789.
[14] Zhang C, Li Y, Cai Y, Shi J, Zheng J, Cai F, Qi H. Parameterization of nearshore wave breaker index. Coastal Engineering. 2021 Sep 1;168:103914.
[15] Lee UJ, Cho HY, Lee BW, Ko DH. Joint probability distribution of significant wave height and peak wave period using gaussian copula method. Journal of Coastal Research. 2024 Jan 15;116(SI):96-100.
[16] "Shore protection manual" (1984), U.S.Army Coastal Engineer Waterways Station,Vicksburg, MS, 2 Volumes, 4^{th} Edition.
[17]- "Coastal Engineering Manual" (2003), Chapter II -2: "Meteorology and Water Climate",Engineer Manual 1110-2-1100, U.S. Army Corps of Engineers, Washington,DC.
[18] Pakhirehzan M, Rahbani M, Malakooti H. Numerical Study of Winter Shamal Wind Forcing on the Surface Current and Wave Field in Bushehr's Offshore Using MIKE21. International Journal Of Coastal, Offshore And Environmental Engineering (ijcoe). 2018 Jul 1;3(2):57-65.
[19] Wang C, Li S, Yu H, Wu K, Lang S, Xu Y. Comparison of wave spectrum assimilation and significant wave height assimilation based on Chinese-French oceanography satellite observations. Remote Sensing of Environment. 2024 May 1;305:114085.
[20] Ahmadvand, H., Paeen Afrakoti, I., Akbari Nasab, M. Comparison of wave prediction methods in Amirabad port. International Journal Of Coastal, Offshore And Environmental Engineering(ijcoe), 2024; (): -. doi: 10.22034/ijcoe.2024.341132.0
[21] Kotaška S, Duchan D, Pelikán P, Špano M. Spectral analysis of oscillatory wind wave parameters in fetch-limited deep-water conditions at a small reservoir and their prediction: Case Study of the Hulín Reservoir in the Czech Republic. Journal of Hydrology and Hydromechanics. 2024;72(1):95-112.
[22] U.S. Army Coastal Engineering Research Center 1977 Shore protection manual. Fort Belvoir, VA, 3 Volumes, 3th Edition.
[23] Mahmoud M, Salameh T, Al Makky A, Abdelkareem MA, Olabi AG. Case studies and analysis of wind energy systems. InRenewable Energy-Volume 1: Solar, Wind, and Hydropower 2023 Jan 1 (pp. 363-387). Academic Press.
[24] Massel, S.R. 1955 Ocean Surface Waves: Their Physics and Prediction, WORLD SCIENTIFIC, Pub.
[25] Rubert, T. 2006 Waves and Waves Forces on Coatal and Ocean Structures. Vol. 21.
[26] Zheng Z, Dong G, Dong H, Ma X, Tang M. Research on the methods for separating wind sea and swell from directional wave spectra in finite-depth waters. Ocean Dynamics. 2024 Feb;74(2):113-31.
[27] Marghany M. Synthetic aperture radar imaging mechanism for oil spills. Gulf Professional Publishing; 2019 Aug 21.
[28] Mazaheri et al have also shown that the wave coefficients can be modified and the use of modified wave coefficients can be used to express the wave behavior in the northern waters of the Persian Gulf with higher accuracy (Mazaheri and Arabzadeh 2015).
[29] Shamshirband S, Mosavi A, Rabczuk T, Nabipour N, Chau KW. Prediction of significant wave height; comparison between nested grid numerical model, and machine learning models of artificial neural networks, extreme learning and support vector machines. Engineering Applications of Computational Fluid Mechanics. 2020 Jan 1;14(1):805-17.
[30] Boyd SC, Weaver RJ. Replacing a third-generation wave model with a fetch based parametric solver in coastal estuaries. Estuarine, Coastal and Shelf Science. 2021 Apr 5;251:107192.
[31] Najarpoor M A, Chegini V, Sadrinasab M. Characteristics of wind wave spectrum in Asalouye region. Jurnal of Marine Sience and Techlogy, 2013 March. 11(4): 57-63.

Appendix

Tabel 1: Empirical equation to prediction wave

method	Minimum time necessary for fetch limited condition	Wave height and wave period
SMB	$\frac{gt_{min}}{U} = 6.5882\, exp\left\{A^{0.5} + 0.8798\left(ln\left(\frac{gX}{U^2}\right)\right)\right\}$ $A = 0.0161\left(ln\left(\frac{gX}{U^2}\right)\right)^2 - 0.3692\left(ln\left(\frac{gX}{U^2}\right)\right) + 2.2024$	$\frac{gH_s}{U^2} = 0.283\tanh\left[0.125\left(\frac{gX}{U^2}\right)^{0.42}\right]$ $\frac{gT_s}{2\pi U} = 1.20\tanh\left[0.077\left(\frac{gX}{U^2}\right)^{0.25}\right]$
Jonswap	$t_{min} = 65.5\frac{X^{0.67}}{g^{0.33}U_{10}^{0.33}}$	$H_{mo} = 0.0016\frac{U_{10}\, X^{0.5}}{g^{0.5}}$ $H_p = 0.286\frac{U_{10}^{0.33}\, X^{0.33}}{g^{0.67}}$
SPM	$\frac{gt_{min}}{U_A^2} = 6.88\times 10^{1}\left(\frac{gX}{U_A^2}\right)^{\frac{2}{3}}$	$\frac{gH_{mo}}{U_A^2} = 1.6\times 10^{-3}\left(\frac{gX}{U_A^2}\right)^{\frac{1}{2}}$ $\frac{gT_p}{U_A} = 2.857\times 10^{-1}\left(\frac{gX}{U_A^2}\right)^{\frac{1}{3}}$
CEM	$t_{x,u} = 77.23\frac{X^{0.67}}{U_{10}^{0.34}\, g^{0.33}}$	$\frac{gH_{mo}}{U_*^2} = 4.13\times 10^{-2}\left(\frac{gX}{U_*^2}\right)^{\frac{1}{2}}$ $\frac{gT_p}{u_*} = 0.751\left(\frac{gX}{u_*^2}\right)^{\frac{1}{3}}$

Table 2: Spectral equation to prediction wave

spectrum	Equation of spectrum	description
Jonswap	$S(f)=\alpha H_s^2\ f_p^4\ f^{-5}\ exp\left[-\frac{5}{4}\left(\frac{f_p}{f}\right)\right]^4$	$\alpha \approx \frac{0.0624}{0.23+0.0336\gamma-\left(\frac{0.185}{1.9+\gamma}\right)}$ $\sigma=\begin{cases}\sigma_a=0.07 & f<f_p\\ \sigma_b=0.09 & f>f_p\end{cases}$ $T_p=\frac{T_s}{\left(1-0.132\gamma^2-0.559\right)}$
Pierson-Moskowitz	$S(f)=\frac{5}{16}H_s^2\ f_p^4\ f^{-5}\ exp\left[-\frac{5}{4}\left(\frac{f_p}{f}\right)^4\right]$	$T_p=1.4\overline{T}$
Mitsuyasu	$S(f)=\frac{1.15\times10^{-4}}{\left(\frac{gF}{U_{10}^2}\right)^{0.312}}\frac{g^2}{f^5}exp\left[-0.99.6\left(\frac{gF}{U_{10}^2}\right)^{-1.23}\left(\frac{U_{10}f}{g}\right)^{-4}\right]$	$k=\frac{gF}{u^2}$
ISSC	$S(w)=5\frac{m_o}{w_p}\left(\frac{w_p}{w}\right)^2 exp\left[-\frac{5}{4}\left(\frac{w_o}{w}\right)^4\right]$	$m_o=0.0625H_s^2$ $w_p=0.7714\,\overline{w}$
Bretschneider	$S(T)=0.43\left(\frac{\overline{H}}{gT^2}\right)^2\frac{g^2}{f^5}exp\left[-0.675\left(\frac{1}{\overline{T}\ f}\right)^4\right]$	-------